



Statistical Validation of GNSS Radio Occultation data over Egypt

Hala. E. A^{1*}, Ashraf E. Mousa², A. Mahrous¹, M. Youssef¹

¹Physics Department, Space Weather Monitoring Centre (SWMC), Faculty of Science, Helwan University;

²National Research Institute of Astronomy and Geophysics (NRIAG)

ARTICLE INFO

Article history:

Received 18 July 2023

Accepted 12 January 2024

Available online 31 January 2024

doi: [10.21608/ABAS.2024.223245.1024](https://doi.org/10.21608/ABAS.2024.223245.1024)

Keywords: GPS radio occultation; Radiosonde; Water vapor distribution.

ABSTRACT

Radiosonde (RS) measurements of the upper atmosphere have long been the principal data source, with measurements spanning more than 60 years. RS has a limited number of stations in Egypt. Thus; it has the poor spatial and temporal resolution, and This negatively affects meteorological research, atmospheric observation, and weather forecasting studies over Egypt. We need to find an additional technique characterized by the length of the available time series and with the high vertical resolution. Global Positioning System Radio Occultation (GPS RO) is the satellite technique received by a low-Earth orbiting satellite to profile earth's atmosphere with high vertical resolution and global coverage. This technique been found to enhance weather forecasting and climate monitoring; In this study, the GPS RO temperature and vapor pressure profiles of the COSMIC satellite mission over Egypt from 2007 to 2019 been validated with those of the available six Radiosonde stations (RS); GPS RO and RS profiles collocated by matching the position and the time, The horizontal distance between the chosen RS stations and the GPS RO event is within 150 km, and the time window was 3 hours; The comparison was performed only on the standard pressure level. One of the objectives of this paper is to check the accuracy of the GPS RO at different elevations; For this aim, the differences between RS and GPS RO were sorted according to pressure level in 4 groups; It is found from the results that GPS RO profiles agree well with RS data; The mean temperature bias for all stations is equal (0.22) with a standard deviation (1.83); On the other hand, mean vapor pressure bias is equal (-0.02) with standard deviation (0.12); According to pressure level sorting, the change of temperature means bias and standard deviation increases with the pressure level decreasing.

1. Introduction

Climate change is one of the most critical problems of our day, faced by the international communities affecting billions of lives and livelihoods[1]. According to studies; global warming has been a significant concern over the past decades and is likely to continue in the future[2]. In the last five decades; human activities have resulted in the release of

increasing greenhouse gases; thus contributing to global climate change by additional heating of the atmosphere[3]. Climate is also affected by our atmosphere, a layer of gases surrounding the earth; These gases wrap around the globe like a blanket, keeping the sun's heat within our atmosphere. The gases that trap the most heat are greenhouse gases because they enable heat to reach the earth; but prevent it

* Corresponding author E-mail analolo_83@yahoo.com

from escaping, much like a greenhouse [4]. Weather and climate studies need high-quality, and high-resolution atmospheric data (i.e., temperature, pressure, humidity, and wind).

Radiosonde (RS) observations have provided the only long-term global in situ measurements of atmospheric pressure, temperature, and humidity in the troposphere and lower stratosphere since 1958 [5]. RS has been the backbone observation system for numerical weather prediction and climate monitoring; and because RS sensor characteristics are modified by the changing environment, measurement accuracy for different sensor types varies significantly over time and location. [5, 6]. It is currently difficult to characterize atmosphere's spatial and temporal variability due to a lack of humidity benchmarks [7].

Global Positioning System Radio Occultation (GPS RO) is a satellite technique that provides high-vertical-resolution and high accuracy refractivity, temperature, and water vapor profiles. The mechanism for obtaining these profiles can be explained simply as a radio signal from a GPS satellite transmitter located in Medium Earth Orbit (MEO) passes through the limb of the atmosphere, is delayed. The bending of radio signals transmitted by GPS satellites as they set or rise behind the earth be measured by installing a GPS receiver onboard a low earth-orbiting (LEO) satellite. Vertical profiles of air refractivity be calculated using bending angle measurements [8].

During the GPS RO event, the Transmitter satellite sets or rises with respect to the receiving satellite, and the radio wave between them are delayed and have a slight frequency shift (Doppler shift); this frequency shift is measured by the receiver and converting it to a parameter called bending angle; the profile of the refractive index can be derived from the profile of bending angle. The GPS RO event takes one minute to profile the earth's atmosphere. [9].

The collaboration Taiwan and USA satellite program (COSMIC) Constellation Observing System for Meteorology, Ionosphere and Climate launched in April 2006; this constellation orbits the earth at 800 km altitude and is considered a low earth orbiter (LEO). The system is composed of six micro-satellites; COSMIC data offers a unique source of meteorological data that gives detailed information about the earth's atmosphere, and improves atmospheric analyses and predictions [10].

FORMOSAT-7/COSMIC-2 (COSMIC- 2) mission launched after the success of cosmic1 (Yue et al., 2014). COSMIC- 2 was successfully launched into low-inclination orbits on 25 June 2019. It has a much higher Signal-to-Noise ratio (SNR) compared to other (RO) missions [5].

This paper aims to achieve the accuracy of the GPS RO and its use in exploring the earth's atmosphere, so in this paper, the GPS RO temperature and vapor pressure profiles of the COSMIC satellite mission over Egypt from 2007 to 2019 been validated with those of the available six RS stations over Egypt.

Previous studies have been done to validate the

temperature and vapor pressure profiles of GPS RO technique with RS [10:22].

Ware et al. (1996) compared 11 temperature profiles derived from GPS/MET soundings with nearby radiosonde and high-resolution balloon soundings; these comparisons show that the accuracy of GPS RO temperature profiles was about 1 K in the lower troposphere. The first global estimate for accuracy of tropospheric water vapor derivations from GPS RO was calculated as a function of height, and a review of the GPS RO technique be found in Kursinski et al. (1995) and Kursinski et al. (1997). According to Rocken et al. (1997) reported that GPS RO observations are all-weather, self-calibrating, and have the significant contribution to a world observing system and enhancing weather prediction and climate research. Rossiter. (2003), and Kuo et al., (2005) confirmed that the RO technique is accurate for measuring atmospheric properties and has high enough accuracy in identifying differences in performance of various types of radiosonde systems.

Temperature and water vapor profiles from CHAMP satellite mission compared with those calculated from radiosonde soundings over Western Australia in Zhang et al. (2007). Results showed that the temperature difference between RO and RS was less than 1 k for altitudes below 14 km and less than 3 k for altitudes near the tropopause. For water vapor profiles, the difference is less than - 0.4 hPa in the lower troposphere, while in the high troposphere, it is less than +0.4 hPa. Kishore et al. (2011) investigated the global distribution of water vapor by COSMIC GPS RO, and a comparison with RS been made. It found that COSMIC GPS RO wet profiles are accurate up to 7–8 km.

Wang et al. (2013) verified the COSMIC RO sounding system using the global RS data, the distance between the RS station and the occultation event is within 100 km horizontally. The time window is 1 hr, the comparison made between 925 and 10 hPa, according to their findings the global mean temperature bias was -0.09 K, with a standard deviation (SD) of 1.72 K, the results indicated that the RO temperature data agreed well with the RS data.

The comparison over Antarctica showed in Norman et al. (2014), the results showed good agreement between two techniques with biases less than 0.5 °C, the biases between 500 and 100 hPa were less than 0.25 °C. Xu et al. (2017) compared two techniques over China, and the results showed that the vertical mean biases of temperature, pressure, and vapor pressure are - 0.10 K, 0.69 hPa, and - 0.01 hPa, respectively.

The comparison of 5 different geographic locations of Iran, were studied in Khaniani, (2020), The RO temperature data selected for comparison was 300 km away and 2 hours from RS measurements, in terms of mean bias, and standard deviation, the agreement of GPS RO temperature below 28 km with respective values obtained from RS was 0.5 K and 1.5 K, respectively. Li et al. (2020) evaluated RO moist profiles by comparing measurements from RS stations distributed in different latitudinal bands; for most pressure

levels, mean differences at polar, mid-latitudinal, and tropical stations was within 0.2 K, 0.5 K, and 1 to 0.2 K, respectively, with standard deviations ranging from 1 to 2 K.

It is worth mentioning that there some studies are conducted on the distribution and accuracy of GPS RO technique over Egypt [23:25].

However, Egyptian meteorologists are unfamiliar with the benefits of GPS RO data, and the number of research using this technique is limited. Therefore; it is essential to understand and compare these data using

In this paper, the GPS RO temperature and vapor pressure profiles of the COSMIC satellite mission over Egypt from 2007 to 2019 been validated with those of the available six RS stations. Section 2 represents the data and study area; Then section 3 presents the comparison method. The validation results of the GPS RO and RS presented in section 4. In this part; the differences between GPS RO and RS at different pressure levels will be statistically assessed. Finally, the conclusions summarized in section 5.

2. Data and study area

To measure the accuracy and stability of GPS RO temperature and vapor pressure profiles over Egypt, the COSMIC GPS RO vapor pressure profiles over Egypt (24° to 38° longitude / 21° to 33° latitude) are validated to those measured using six Radiosonde (RS) stations from 2007 to 2019. For this validation the COSMIC GPS RO retrieval product wetPrf profiles and Radiosonde profiles from 2007 to 2019 were used. The wetPrf file is an atmospheric occultation profile that includes meteorological data, such as atmospheric pressure, geometric height, temperature, water vapor pressure, etc. This file gives the data at levels of 100 meters in height. The wetPrf profiles were downloaded from COSMIC Data Analysis and Archive Centre (CDAAC). The data from January 2007 to April 2014 were downloaded from cosmic 1, Reprocessed Datasets (<https://data.cosmic.ucar.edu/gnssro/cosmic1/repro2013/level2/>) and the data from May 2014 to December 2019 were downloaded from cosmic 1, Post-Processed Datasets (<https://data.cosmic.ucar.edu/gnssro/cosmic1/postProc/level2/>). These data provided more than 19000 profiles over Egypt during the study period.

The RS profiles were downloaded from National Oceanic and Atmospheric Administration (NOAA) (which includes RS and atmospheric science observations from globally distributed stations). The RS data of 00:00 and 12:00 UTC were used. The horizontal distances between the chosen RS stations and the GPS RO event are within 150 km and the time window is 3 hours. Six stations of RS were selected for comparison with wetPrf profiles. The stations of RS are shown in different colors in Figure (1). Table (1) presents the geographical characteristics of RS stations used in this

study. It should be noted that the 6 stations are distributed in separate places in Egypt, to cover different climate conditions of Egypt.

3. Comparison method.

For the validation between GPS RO data and RS data, first we reformatted RS files to separate each day to fit our wetPrf files. Second, we compared the coordinates to find the nearest GPS RO events that matched with our stations within the horizontal distances of 150km. Third we compared the nearest time files within time window of 3 hours. The comparison was performed only on the standard pressure level to avoid errors due to interpolation of RS profiles since WetPrf files altitude range was 0–40 km with 100m vertical resolution. On the other hand, the downloaded RS data had a much lower vertical resolution [19]. Water vapor pressure profiles are created from radiosonde temperature, and relative humidity profiles using the following formula:

(<https://www.weather.gov/media/epz/wxcalc/vaporPressure.pdf>)

$$e_s = 6.11 * 10 \exp (at/b+t) \quad (1)$$

where

$$a = 9.5, \quad b = 265.5 \quad \text{for } t > 0$$

$$a = 7.5, \quad b = 237.3 \quad \text{for } t < 0$$

partial vapor pressure (e) in mb was calculated using the next formula: -

$$e = e_s * RH / 100 \quad (2)$$

The analysis was carried out in terms of temperature difference (ΔT), and vaper pressure difference (ΔV_p), which is given by:

$$\Delta T = T_{\text{wet Prf}} - T_{\text{RS}} \quad (3)$$

$$\Delta V_p = V_{p\text{wetPrf}} - V_{p\text{RS}} \quad (4)$$



Fig (1): Spatial distributions of matched Radiosonde

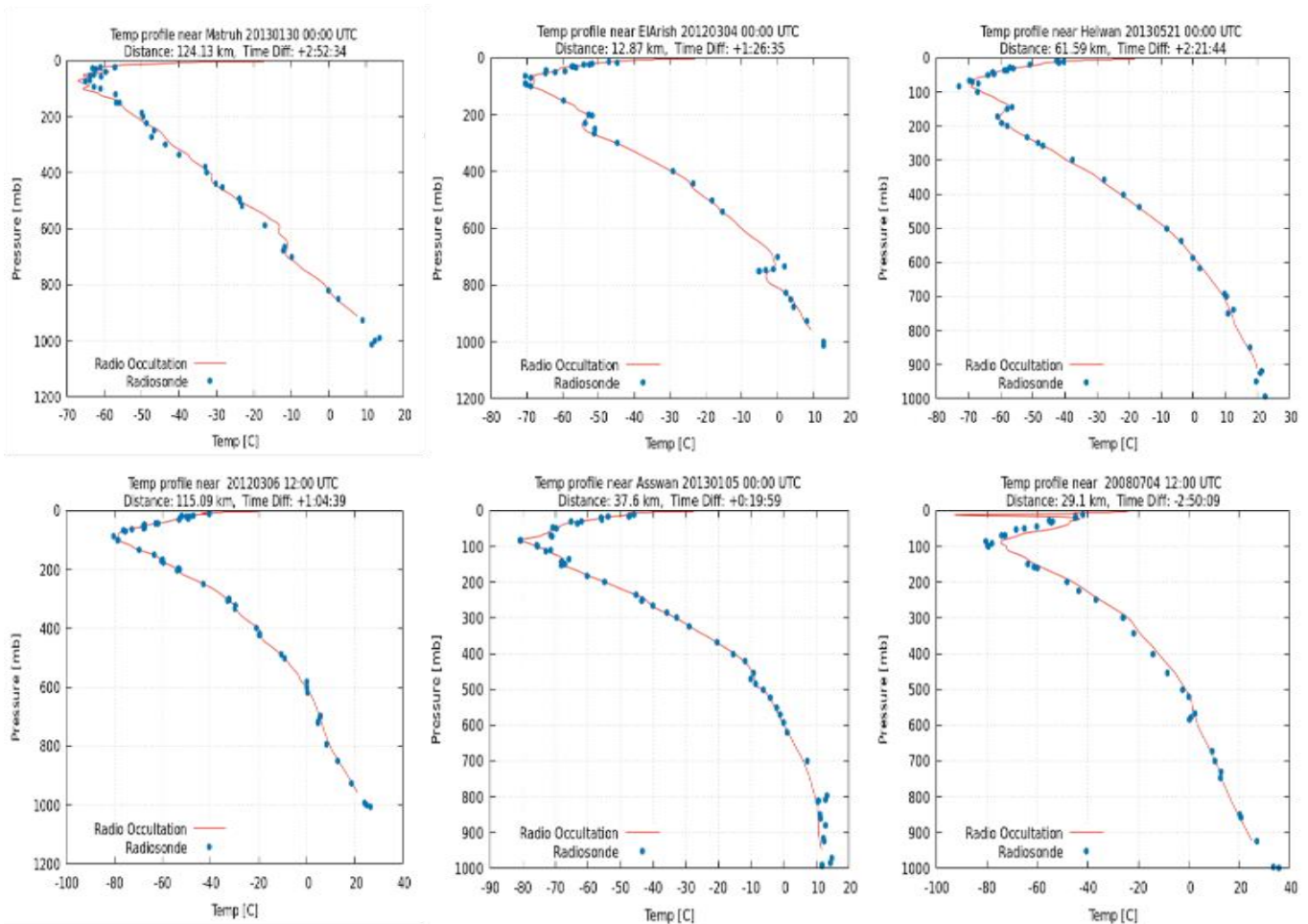


Fig. 2: Validation of temperature and profiles between RS stations and GPS RO data for spatially (150 km) and temporally (± 3 hours) during the period (2007-2019) at Mersa Matruh (62306), Farafra (62423), Aswan (62414), Qena (62403), Helwan (62378), and El Arish (62337) stations over Egypt.

Table (1): Geographic characteristics of radiosonde stations

| Station name | Station Number | Location |
|--------------|----------------|---------------|
| Aswan | 62414 | 23.58N 32.47E |
| El-Arish | 62337 | 31.05N 33.45E |
| Mersa Matruh | 62306 | 31.20N 27.13E |
| Helwan | 62378 | 29.52N 31.20E |
| Qena | 62403 | 26.20N 32.75E |
| Farafra | 62423 | 27.05N 27.96E |

4. Results

4.1 Temperature comparison

Figure (2) shows the comparison of temperature profiles between RS stations and GPS RO data for spatially (150 km) and temporally (± 3 hours) during the period (2007-2019) at Mersa Matruh, Farafra, Aswan, Qena, Helwan, and El Arish stations over Egypt. According to pressure levels, as seen in the figures there is a very good agreement between two techniques, it is clear from the validation of the

temperature profiles that there is high vertical resolution of GPS RO profiles that explains a continuous graph of temperature profiles, and also the figure shows a high density of GPS RO at different pressure levels enables for more accurate temperature monitoring in different levels and provides more information about the atmosphere.

4.2 Temperature histograms

Figure (3) shows relative frequency histograms for temperature bias between available RS stations and GPS RO data during the period (2007-2019) over Egypt.

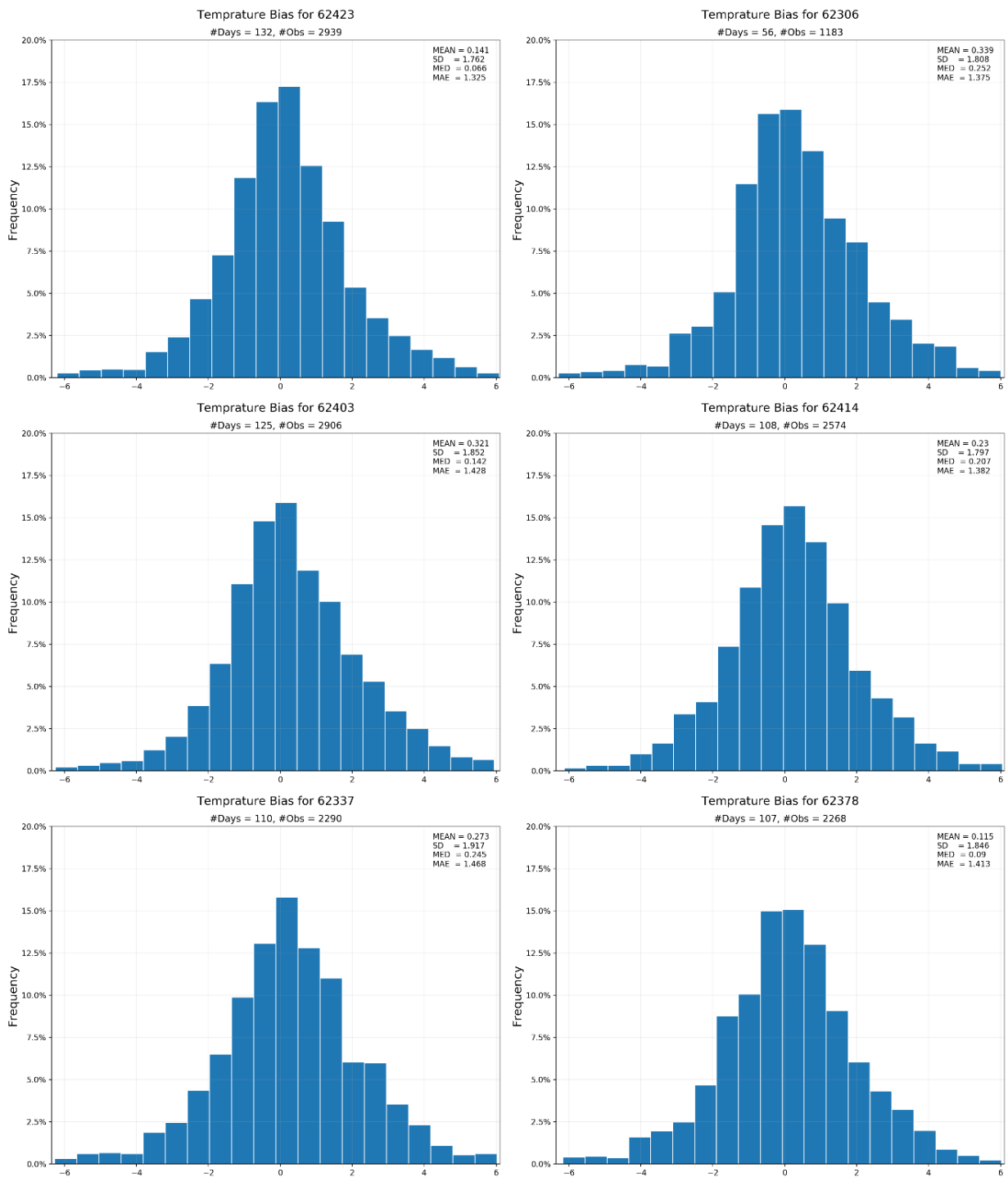


Fig. 3: Relative frequency histograms for temperature bias between RS stations and GPS RO data during the period (2007-2019) at Mersa Matruh (62306), Farafra (62423), Aswan (62414), Qena (62403), Helwan (62378), and El Arish (62337) stations over Egypt.

The figure also shows the statistical analysis such as mean, standard deviation (SD), median (MED), and mean absolute errors (MAE). The X axis in figure (3) represents the temperature bias between RS stations and GPS RO data, and

Y axis represents the relative frequency distribution. From those histograms we can say that most of data are clustered around the center (from zero to ± 1), the shape of the histograms forms a symmetrical bell shape (normally

distributed), and the same pattern occurs for relative frequency histograms of all stations as shown in figure (4). From these results we can see that there is good agreement between the RO and RS data

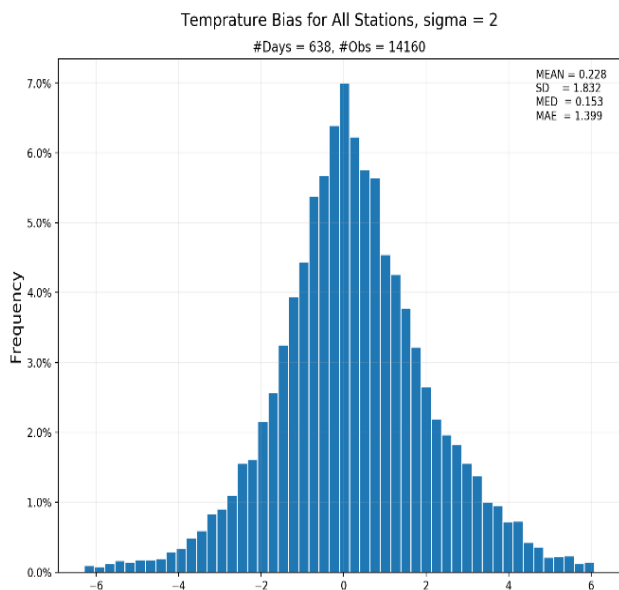


Fig. 4: Relative frequency histograms for temperature bias between RS stations and GPS RO data during the period (2007-2019) at all stations over Egypt.

From those results, the mean of the differences ranges from 0.12 at Helwan, to 0.34 at Mersa Matruh, the median value ranged from **0.07** at Farafra to **0.25** at Mersa Matruh, standard deviations of all stations are grouped around (1.76 – 1.92), and the mean absolute errors values vary from **1.33** at Farafra to **1.47** at El Arish station. The standard deviation and the mean absolute error are high values, this maybe because the RS stations over Egypt have no tracking balloon technique, so in comparison method between RS and RO we found matched days have long track locations and short track locations as shown in the figure (5). The difference of the position of RS and RO, as well as the non-verticality of the RS profiles which amount to about 200 km distance may cause the high values of SD and MAE [21]. Furthermore, the RO profiles are not completely vertical, and the location of tangent points in each profile can vary up to 100 kilometers horizontally. [10].

To clarify that table (1) illustrates the mean, SD, MED, and MAE for long track location and short track location between GPS RO and RS at the days 20070515, and 20071023 respectively for El Arish station, the statistical values have lower values in short track location day than those of the long track location. It is necessary to mention that the high values of SD and MAE doesn't reflect that the GPS RO measurements is not less accurate than RS measurements, but it may be interpreted due to the spatial and temporal variations between matched observations.

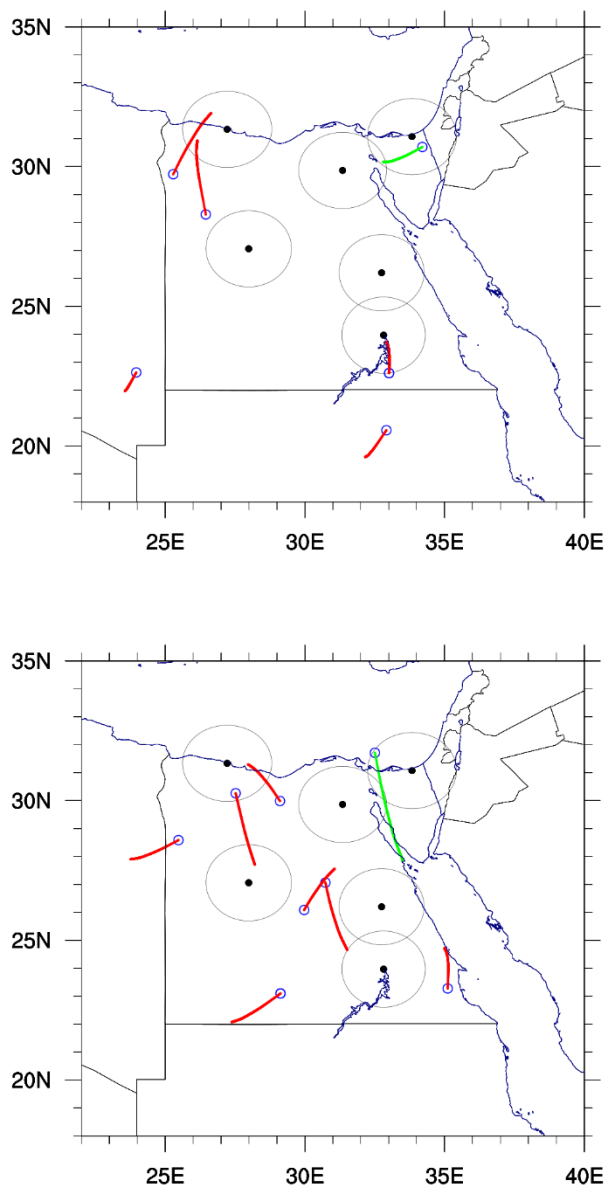


Fig. 5: long track and short track for comparison between RS stations and GPS RO data at the days 20070515, and 20071023 respectively for El Arish (62337) station, the green color is the matched location, and the red color is unmatched location, and the black dots is the RS station locations over Egypt.

4.3 Temperature histograms according to elevation

One of the objectives of this paper is to check the accuracy of the GPS RO at different elevations. For this aim the differences between RS and GPS RO were sorted according to pressure level in to four groups, below 700mb, between 700mb and 300 mb, between 300mb and 100mb, and above 100mb.

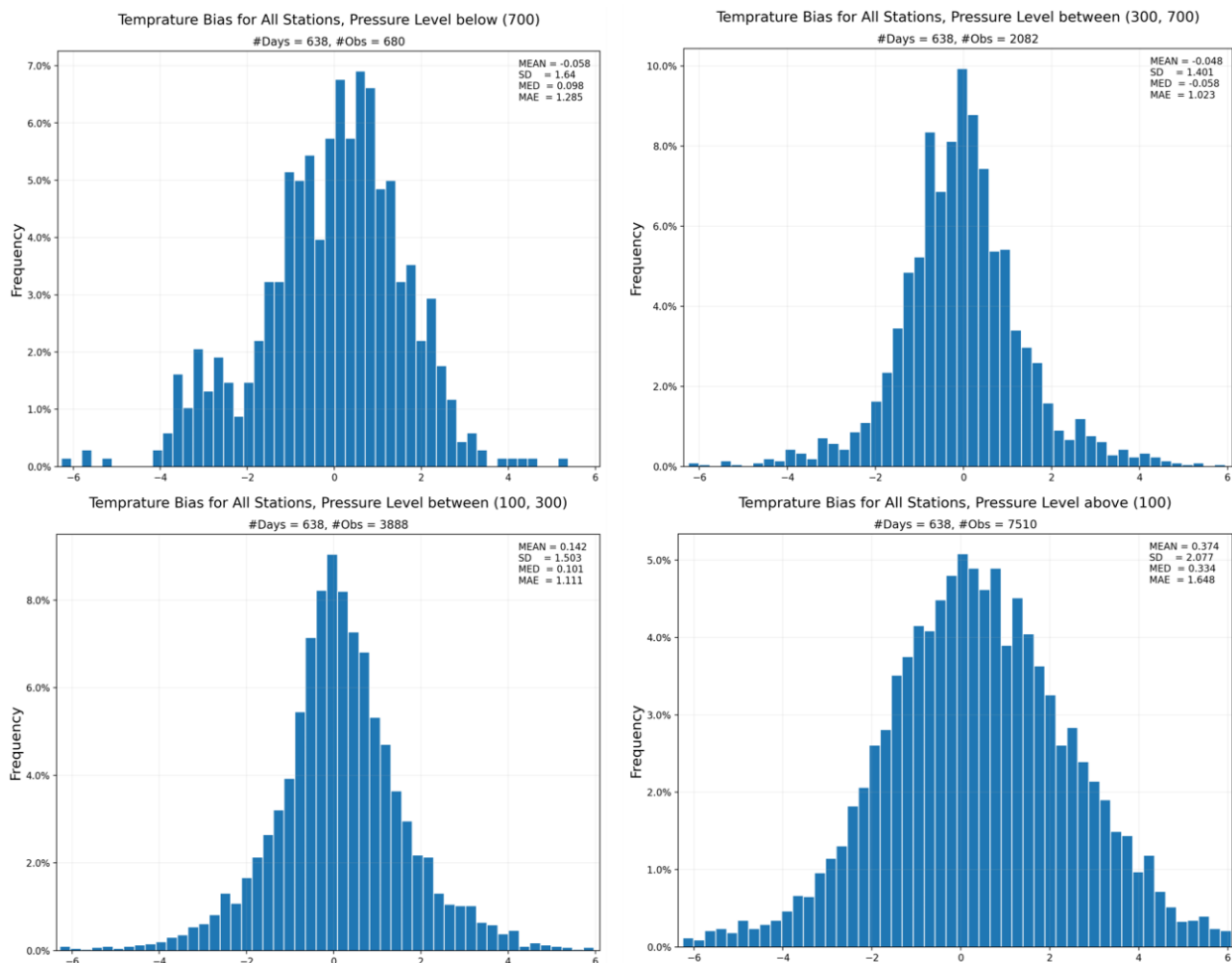


Fig. 6: Relative frequency histograms for temperature bias according to elevations between RS stations and GPS RO data during the period (2007-2019) at all stations over Egypt.

Table 1: Statistical analysis of the difference between the RS and GPS RO temperatures based on long track and short track at the days 20070515, and 20071023 respectively for El Arish (62337) station.

| | Long track 20070515 El Arish (62337) | Short track 20071023 El Arish (62337) |
|------|--|---|
| Mean | 0.94 | 0.039 |
| SD | 1.92 | 1.13 |
| MED | 1.18 | 0.22 |
| MAE | 1.81 | 0.99 |

Figure (6) shows the relative frequency histograms for temperature bias according to elevations between RS stations and GPS RO data during the period (2007-2019) at all stations over Egypt. It's clear that the shapes of

histograms are nearly symmetrical distribution except histogram at pressure levels below 700 mb, probably due to the small number of observations where the number of observations is 638, while the other histograms the number of observations is higher. Figure (6) also illustrates statistical analysis of temperature bias according to elevations between RS stations and GPS RO data during the period (2007-2019) at all stations over Egypt. The results show that there is a tendency to increase of the mean bias with the pressure level decreasing, this might be due to the greater spatial differences between GPS RO events and RS stations as we mentioned above. The median value ranged from 0.05 at the levels between (300mb - 100mb) to 0.18 at the levels (above 100mb), and the mean absolute errors values vary from 0.96 at the levels between (700mb -300mb) to 1.60 at the levels above 100mb. Table (2) shows the relative frequency histograms for temperature bias between RS stations and GPS RO data according to elevations during the period (2007-2019) at individual stations over Egypt.

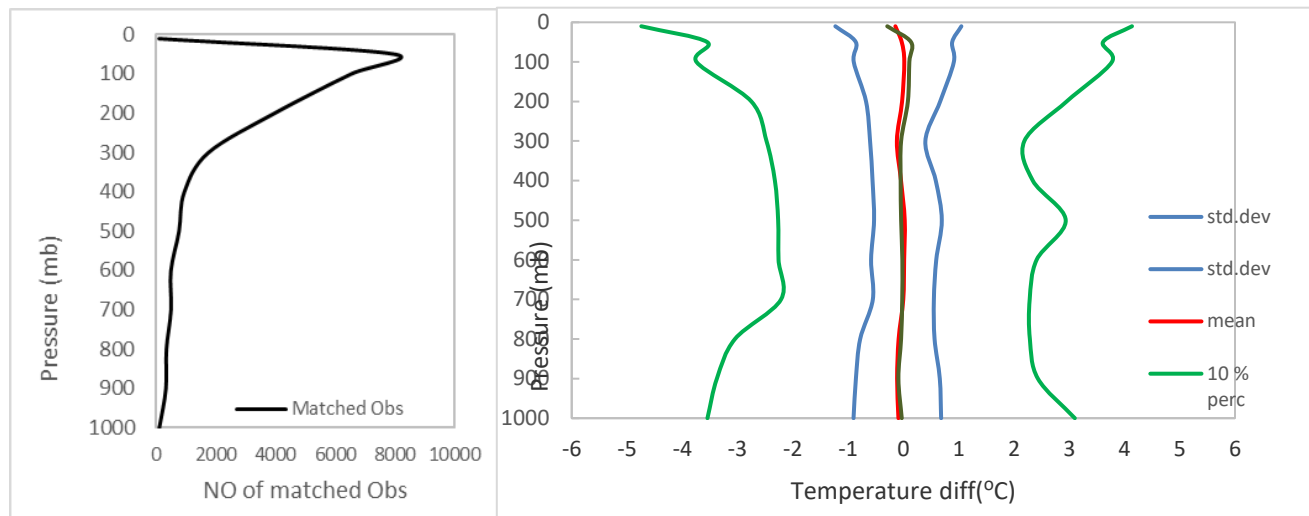


Fig. 7: The overall comparison statistics of temperature differences and the number of matched observations as a function of pressure level is shown for comparison of cosmic mission GPS RO data and RS data at six stations over Egypt from 2007 to 2019.

Table (2): Statistical analysis of temperature bias according to elevations between RS stations and GPS RO data during the period (2007-2019) at individual stations over Egypt.

| | | below 700mb | 700mb -300mb | 300mb - 100mb | above 100mb |
|---------------------------------|------|-------------|--------------|---------------|-------------|
| Mersa Matruh (62306) 56 days | Obs | 76 | 204 | 315 | 588 |
| | Mean | -0.033 | -0.205 | 0.412 | 0.537 |
| | SD | 1.293 | 1.456 | 1.657 | 1.998 |
| | MED | 0.136 | -0.214 | 0.284 | 0.487 |
| | MAE | 1.002 | 1.076 | 1.243 | 1.556 |
| El Arish (62337) 110 days | Obs | 109 | 331 | 665 | 1185 |
| | Mean | -0.098 | 0.084 | 0.219 | 0.390 |
| | SD | 1.895 | 1.522 | 1.684 | 2.121 |
| | MED | 0.249 | 0.032 | 0.224 | 0.389 |
| | MAE | 1.450 | 1.125 | 1.239 | 1.688 |
| Helwan (62378) 107 days | Obs | 113 | 315 | 647 | 1193 |
| | Mean | -0.392 | -0.072 | 0.081 | 0.231 |
| | SD | 1.653 | 1.450 | 1.574 | 2.067 |
| | MED | -0.335 | -0.069 | 0.075 | 0.254 |
| | MAE | 1.295 | 1.026 | 1.184 | 1.640 |
| Qena (62403) 125 days | Obs | 103 | 421 | 775 | 1607 |
| | Mean | 0.002 | -0.122 | 0.104 | 0.562 |
| | SD | 1.499 | 1.358 | 1.422 | 2.111 |
| | MED | -0.008 | -0.138 | 0.021 | 0.559 |
| | MAE | 1.194 | 0.983 | 1.057 | 1.687 |

| | | | | | |
|-----------------------------|------|------------|------------|------------|-------------|
| Aswan (62414) 108 days | Obs | 135 | 372 | 697 | 1370 |
| | Mean | 0.352 | 0.00031 | 0.107 | 0.342 |
| | SD | 1.673 | 1.321 | 1.389 | 2.073 |
| | MED | 0.526 | 0.072 | 0.118 | 0.295 |
| | MAE | 1.327 | 1.004 | 1.047 | 1.655 |
| Farafra (62423) 123 days | Obs | 144 | 439 | 789 | 1567 |
| | Mean | -0.206 | -0.026 | 0.087 | 0.247 |
| | SD | 1.569 | 1.337 | 1.370 | 2.030 |
| | MED | 0.036 | -0.115 | 0.047 | 0.179 |
| | MAE | 1.254 | 0.960 | 0.993 | 1.596 |

From the table we can see that the mean in all stations increases with decreasing pressure levels except in Aswan station where the maximum mean value occurs at the levels below 700mb, and minimum value occurs at the levels between (700mb – 300mb). The reason for this maybe because the small number of observations at Aswan stations at these levels. The standard deviation ranged from (1.32) at the levels (700mb – 300mb) of Aswan station to (2.1) at the levels (above 100 mb) of El Arish station. As for a median, it's between (-0.33) at the levels (below 700mb) of Helwan station, and (0.55) at levels (above 100 mb), and mean absolute error ranges from (0.96 at the levels (between 700mb – 300mb) of Farafra station and (1.68) at the levels (above 100mb). Away from the variable range change at each station, all shows the same trend as the all stations. As shown before in figure (6).

Figure (7) represents the overall comparison statistics temperature differences as a function of pressure level for the comparison of cosmic mission GPS RO data and RS data at available six stations over Egypt from 2007 to 2019. The number of matched observations is shown in the left of the figure. From figure (7) the mean of temperature differences stays below (0.1°C) for most atmospheric pressure levels, the median values also stay below 0.1 except at pressure level (1 – 10 mb) has the value of 0.2, and the standard deviation stay below (1) except at pressure level (1 – 10 mb) has the value of (1.2). From matched observations figure we can notice that the number of matched observations between GPS RO data and RS data at pressure levels (900 -1000 mb) which represent the lower troposphere and at (1 -10 mb) which represent the top layer of atmosphere are less than 120 collocations and this can influence the statistical analysis and makes them high. As for the pressure levels from 900 mb to 50 mb, have high numbers of matched observations reaches up to 8000 observations, and this reduce the values of statistical analysis which carried out.

The small number of matched observations at the top of atmosphere could be because the available RS data is

decreasing in this layer depends on the average height of a balloon burst. And at the lower tropospheric layers include little information from GPS RO data because GPS RO technique does not reach to the surface due to the atmospheric reflection and multipath effects in the lower troposphere. [26].

4.4 Daytime and nighttime temperature differences

In general, there is a good agreement between two techniques, but we need more identification of the reasons for the differences, so that we split the matched observations into daytime (2 p.m.) and nighttime (2. a.m.) to characterize the radiation biases as shown in figure (8). The data from most RS types show a nighttime cold bias and a daytime warm bias. Radiative effects (typically a warm bias during the day from sunlight heating the sensor and a cold bias at night as the sensor emits longwave radiation) cause the most of radiosonde temperature biases, with smaller errors due to lags in sensor response to changing temperatures as the radiosonde rises. [27].

From nighttime work showed in figure (8) the mean of temperature differences stays below (0.1) for most atmospheric pressure levels, the median values also stay below (0.1) except at pressure level (1 – 10 mb) has the value of (0.2), and the standard deviation stay below (1.1).

For the daytime work in figure (8), the mean of temperature differences stays below (0.1) for most atmospheric pressure levels and have negative values from the surface to the pressure level (300 mb), this is mean that the values of GPS RO temperature profiles are lower than those of RS profiles at these pressure levels and vice happens at pressure levels from (200 mb to 10 mb).

The median values also stay below 0.1 except at pressure level (1 – 10 mb) has the value of (0.4), and the standard deviation stay below (1) except at pressure level (1 – 10 mb) has the value of (2.1).

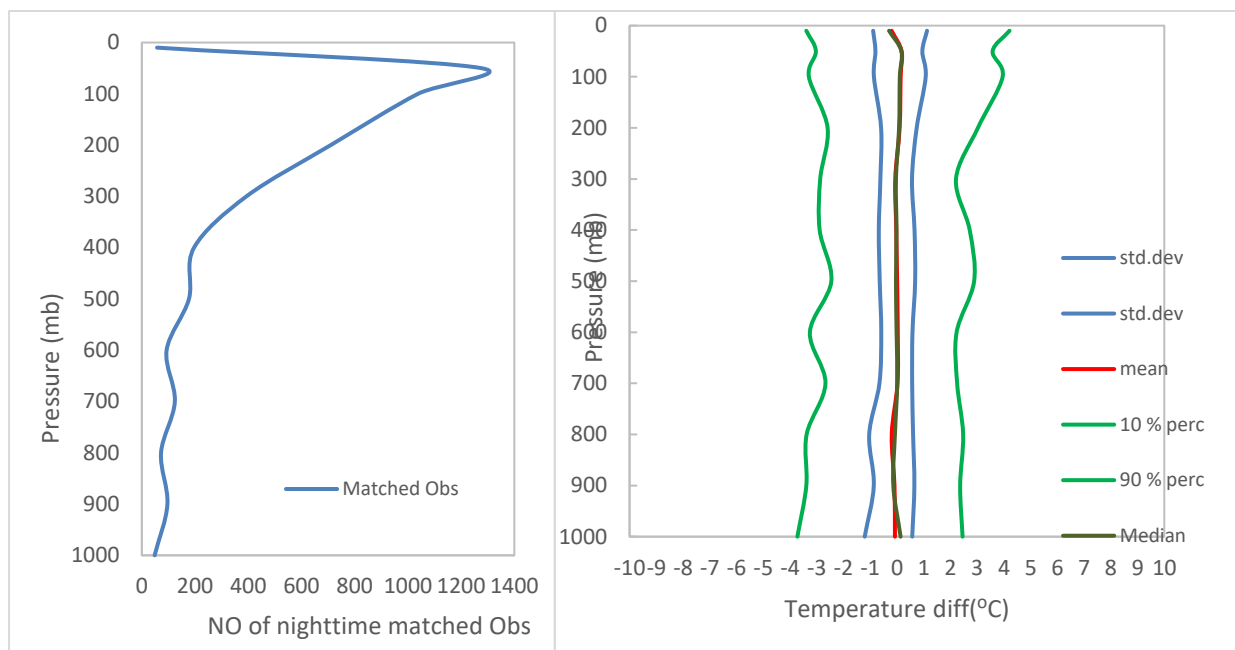


Fig. 8: The daytime and nighttime statistics of temperature differences and the number of matched observations as a function of pressure level for comparison of cosmic mission GPS RO data and RS data at available six stations over Egypt from 2007 to 2019.

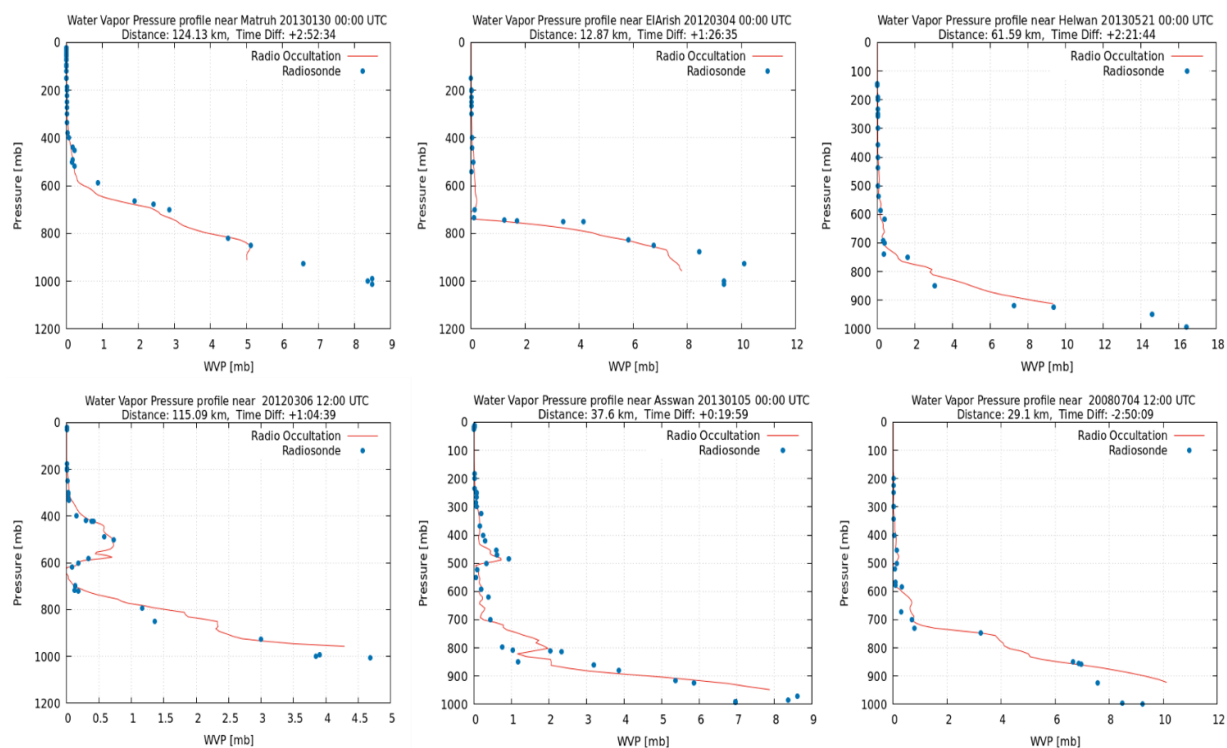


Fig. 9: Validation of vapor pressure and profiles between RS stations and GPS RO data for spatially (150 km) and temporally (± 3 hours) during the period (2007-2019) at Mersa Matruh (62306), Farafra (62423), Aswan (62414), Qena (62403), Helwan (62378), and El Arish (62337) stations over Egypt.

4.5 Vapor pressure comparison.

From the validation of vapor pressure profiles which shown in figure (9), there is a very good agreement between two techniques as we mentioned above, but it's obvious that the GPS RO measurement has an issue in the lower troposphere because not all the RO profiles penetrate down to the surface thus the uncertainty of GPS RO measurements increases in this layer especially in the planetary boundary layer (PBL) owing to the topographic blockage of RO signals reaching the Earth's surface, Furthermore the corruption of RO signal is rising receiver tracking inaccuracy. [28]. Also, from figure we can notice that in the upper tropopause and stratosphere, where the effects of water vapor are insignificant, the difference between the two techniques is very small, nearly zero.

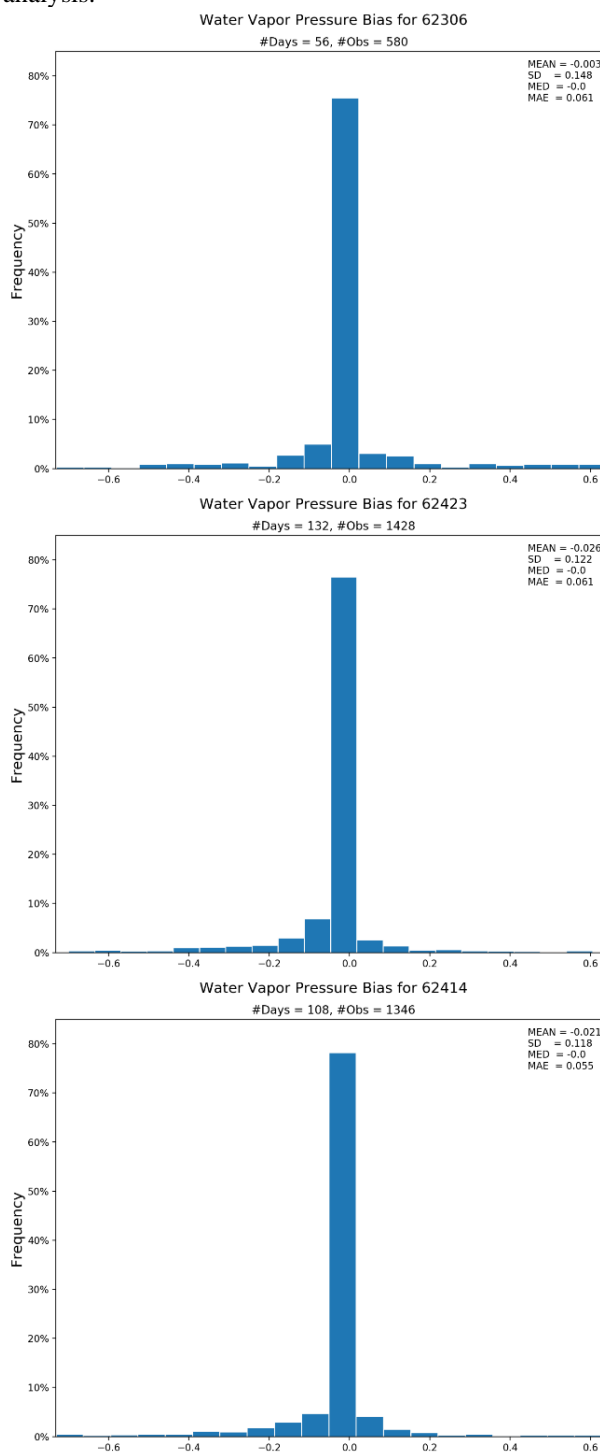
4.6 Vapor pressure histograms

Figure (10) shows relative frequency histograms for vapor pressure bias between RS stations and GPS RO data during the period (2007-2019) at available six stations over Egypt. As the relative frequency histograms for temperature bias, most of data are clustered around Zero, and the shape of the columns forms a symmetrical bell shape (normally distributed), and the same pattern occurs for relative frequency histograms of all stations as shown in figure (11). from the figure we can see that all statistical values are very close to zero, and the mean vapor pressure bias have a negative value, this is means that the GPS RO vapor pressure values are lower than of those in RS measurements. In general, the small variation of statistical analysis indicated that the vapor pressure of RS and GPS RO agree very well.

4.7 Vapor pressure histograms according to elevation

Figure (12) shows the relative frequency histograms for vapor pressure bias according to elevations between RS stations and GPS RO data during the period (2007-2019) at six stations over Egypt. it's clear that the shapes of histograms are nearly symmetric distribution except at pressure levels below 700 mb, probably due to the small number of observations where the number of observations is 246 in comparison to the number of observations of the other histogram. And as we mentioned above that the difference between two techniques in the upper tropopause and in the stratosphere are very close to zero where the effect of water vapor is negligible, so that the graphs at (between 300mb: 100mb) and below 100mb show no variation. Table (3) shows the relative frequency histograms for vapor pressure bias between RS stations and GPS RO data according to elevations during the period (2007-2019) at six stations over Egypt. For all stations, the mean biases and median differences values are very close to zero. The standard deviations decrease with the increase of height with values (0.3 ,0.4) at below 700 mb and value around (0.2) between

(700mb :300mb). The mean absolute errors values are also close to zero except at the level below 700mb this is because the small number of observations. In general, from the above results the GPS RO vapor pressure profiles agree very well with those from RS in different regions over Egypt. This is indicated by relatively smaller variation of the statistical analysis.



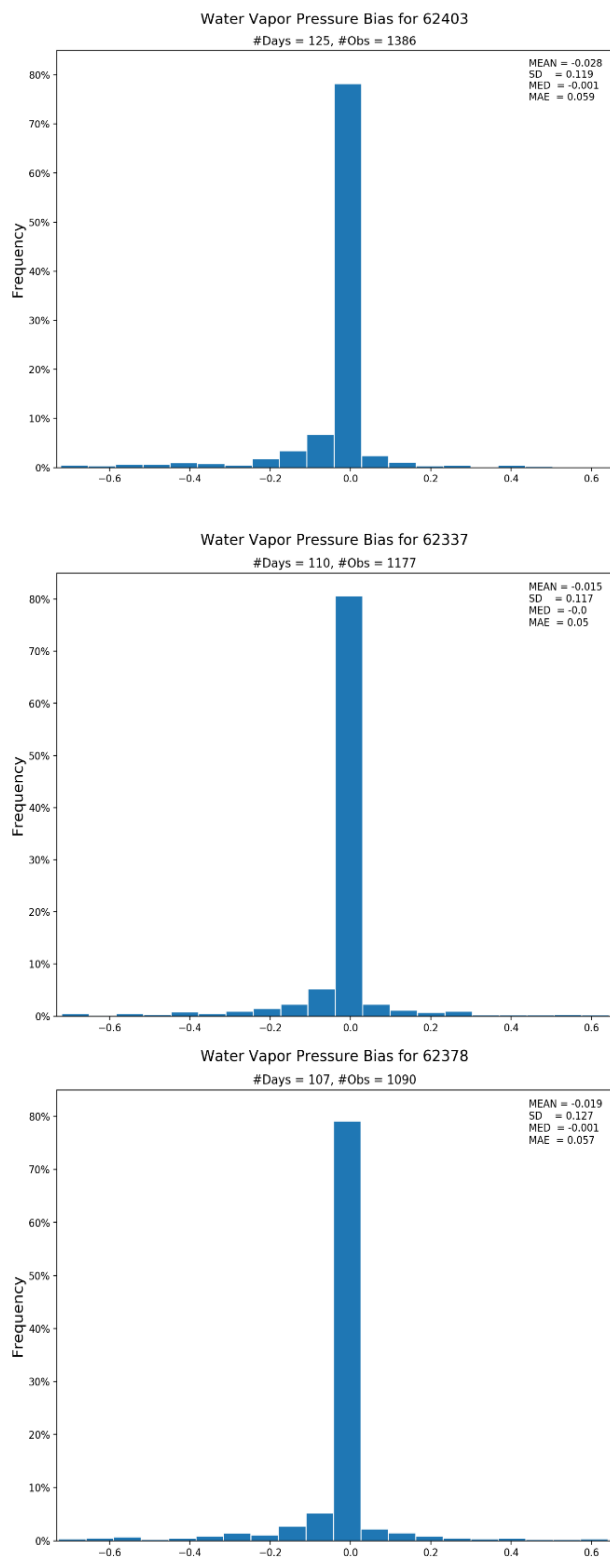


Fig. 10: Relative frequency histograms for vapor pressure bias between RS stations and GPS RO data during the period (2007-2019) at Mersa Matruh (62306), Farafra (62423), Aswan (62414), Qena (62403), Helwan (62378), and El Arish (62337) stations over Egypt.

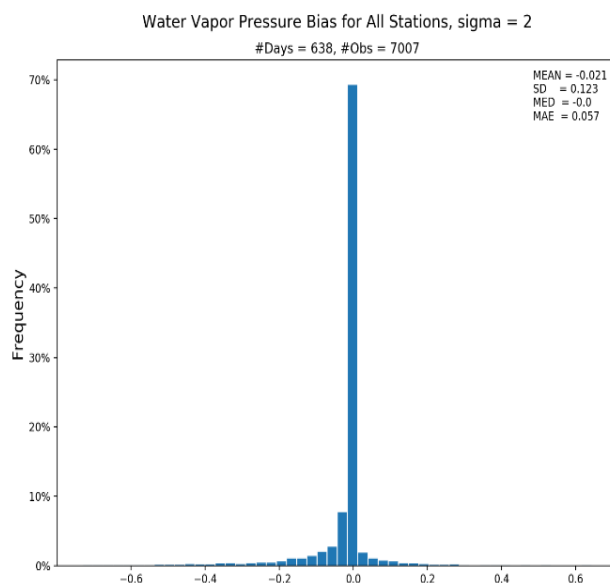


Fig. 11 : Relative frequency histograms for vapor pressure bias between RS stations and GPS RO data during the period (2007-2019) at all stations over Egypt.

Figure (13) represents the overall comparison statistics vapor pressure differences as a function of pressure level for the comparison between two techniques at available six stations over Egypt from 2007 to 2019. From figure we can see that the mean of vapor pressure differences stays below (0.01°C) for all atmospheric pressure levels except at the surface at pressure level (900 – 1000 mb) has the value (0.1) due to small number of observations as mentioned above, the median values are very small and very close to zero, and the standard deviation stay below (0.9) except at surface has the value of (1.4).

4.8 Daytime and nighttime vapor pressure differences

Figure (14) represents the daytime and nighttime statistics of vapor pressure differences and the number of matched observations. For the daytime work in figure (14) the mean vapor pressure differences are very close to zero for all atmospheric pressure levels, the median values are stay below (0.01) at all pressure levels except at the surface which has the value of 0.1, and the standard deviation stay below (0.9) except at surface has the value of (1.5).

And from nighttime work the mean vapor pressure differences stay below (0.1) for all atmospheric pressure levels except at the surface at pressure level (900 – 1000 mb) which has the value of (0.3) due to small number of observations as mentioned above, the median values are also stay below (0.1), and the standard deviation stay below (1) except at surface has the value of (1.8).

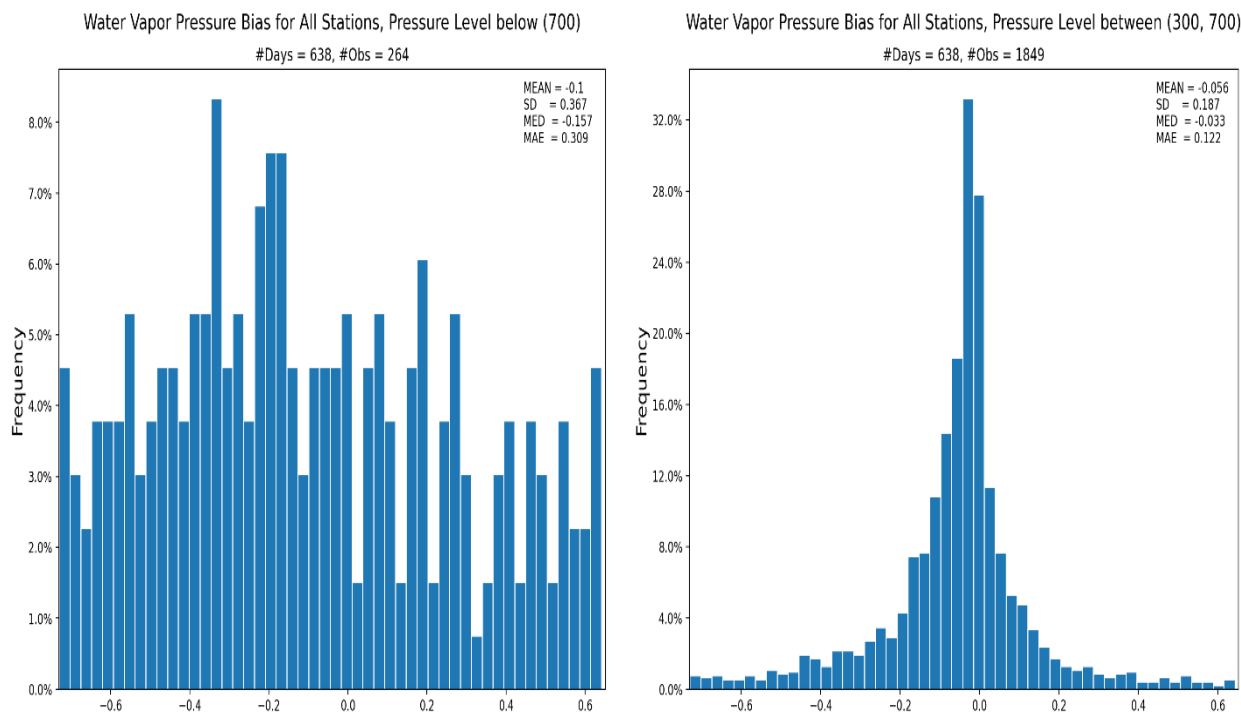


Fig. 12: Relative frequency histograms for vapor pressure bias according to elevations between RS stations and GPS RO data during the period (2007-2019) at all stations over Egypt.

Table (3): Statistical analysis of vapor pressure bias according to elevations between RS stations and GPS RO data during the period (2007-2019) at individual stations over Egypt.

| | | below 700mb | 700mb -300mb | 300mb - 100mb | above 100mb |
|---------------------------------|------|-------------|--------------|---------------|-------------|
| Mersa Matruh (62306) 56 days | Obs | 29 | 184 | 314 | 171 |
| | Mean | 0.057 | -0.016 | -0.003 | -2.23E-05 |
| | SD | 0.421 | 0.200 | 0.005 | 2.79E-04 |
| | MED | 0.163 | -0.033 | -0.004 | -1.12E-04 |
| | MAE | 0.374 | 0.125 | 0.003 | 2.03E-04 |
| El Arish (62337) 110 days | Obs | 40 | 296 | 452 | 389 |
| | Mean | -0.171 | -0.031 | -0.004 | 4.25E-05 |
| | SD | 0.325 | 0.190 | 0.007 | 3.97E-04 |
| | MED | -0.262 | -0.038 | -0.004 | -8.79E-05 |
| | MAE | 0.277 | 0.116 | 0.004 | 2.74E-04 |
| Helwan (62378) 107 days | Obs | 43 | 301 | 441 | 305 |
| | Mean | -0.084 | -0.050 | -0.004 | 8.3E-05 |
| | SD | 0.369 | 0.191 | 0.008 | 6.5E-04 |
| | MED | -0.141 | -0.041 | -0.004 | -1.2E-04 |
| | MAE | 0.307 | 0.121 | 0.005 | 3.6E-04 |

| | | | | | |
|-----------------------------|------|--------|----------|--------|-----------|
| Qena (62403) 125 days | Obs | 41 | 348 | 460 | 537 |
| | Mean | -0.101 | -0.091 | -0.008 | 4.4E-05 |
| | SD | 0.371 | 0.183 | 0.011 | 4.3E-04 |
| | MED | -0.156 | -0.069 | -0.006 | -9.0E-05 |
| | MAE | 0.308 | 0.126 | 0.008 | 3.1E-04 |
| Aswan (62414) 108 days | Obs | 55 | 337 | 472 | 483 |
| | Mean | -0.156 | -0.05048 | -0.005 | 0.00018 |
| | SD | 0.359 | 0.171 | 0.014 | 0.00060 |
| | MED | -0.178 | -0.048 | -0.005 | -0.00002 |
| | MAE | 0.301 | 0.114 | 0.007 | 0.00037 |
| Farafra (62423) 123 days | Obs | 56 | 383 | 466 | 523 |
| | Mean | -0.089 | -0.075 | -0.008 | 6.19E-05 |
| | SD | 0.341 | 0.184 | 0.012 | 4.35E-04 |
| | MED | -0.116 | -0.067 | -0.006 | -1.02E-04 |
| | MAE | 0.275 | 0.124 | 0.008 | 3.22E-04 |

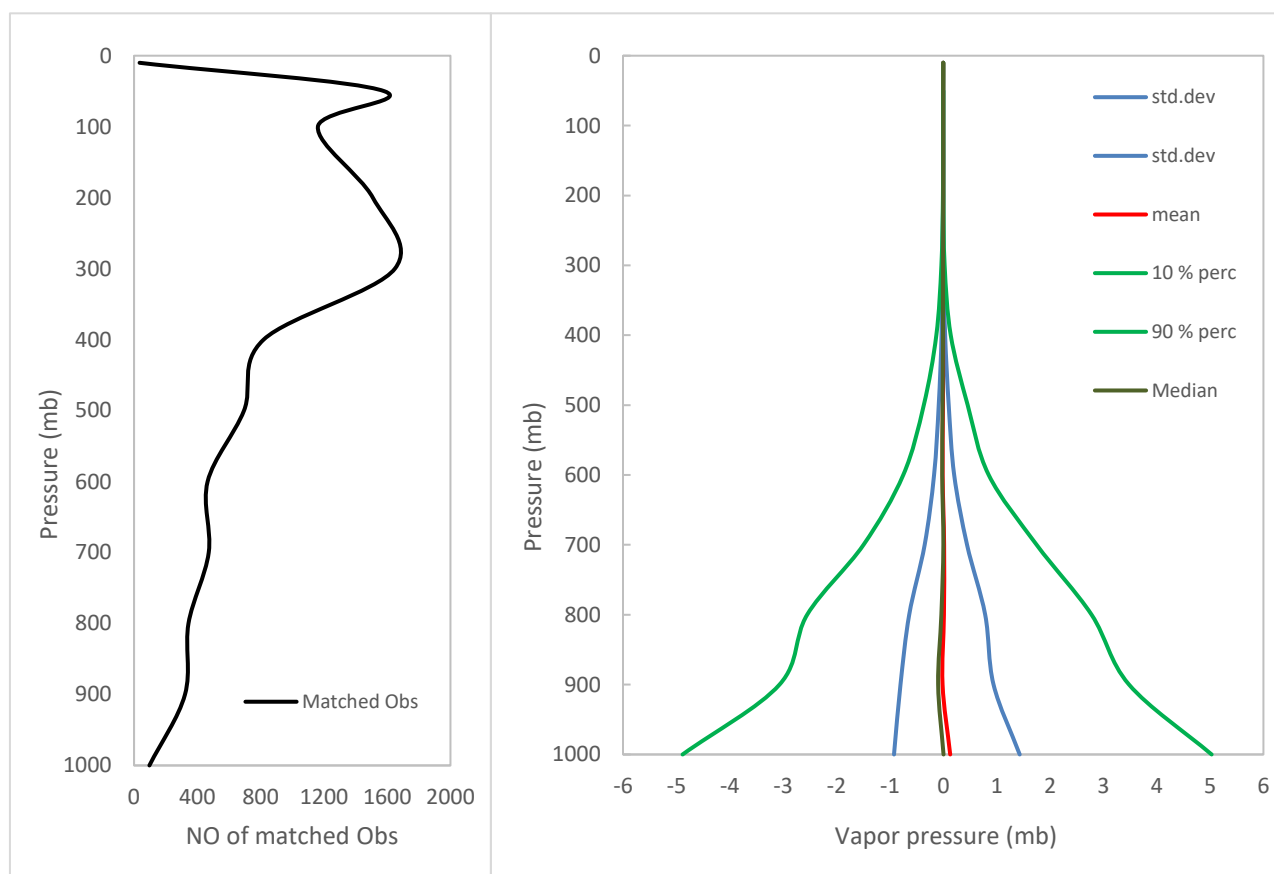


Fig. 13: The overall comparison statistics of vapor pressure differences and the number of matched observations as a function of pressure level is shown for comparison of cosmic mission GPS RO data and RS data at six stations over Egypt from 2007 to 2019.

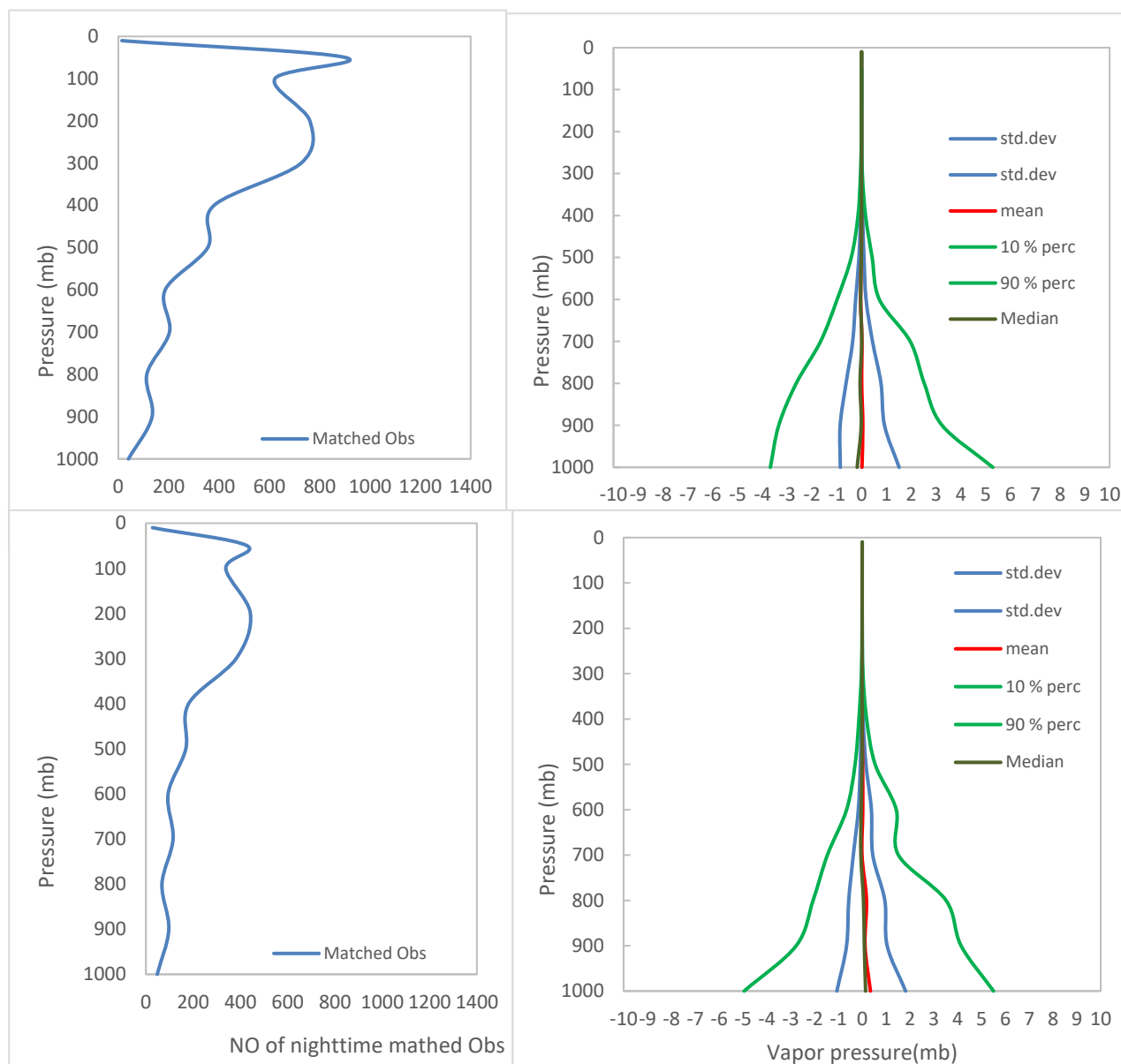


Fig. 14: The daytime and nighttime statistics of vapor pressure differences and the number of matched observations as a function of pressure level for comparison of cosmic mission GPS RO data and RS data at available six stations over Egypt from 2007 to 2019.

Conclusions

The meteorological research, atmospheric observation, and weather forecasting studies need a continuous, accurate, and stable observation of atmospheric temperature and vapor pressure with a sufficient temporal and spatial resolution. The accessibility of GPS RO data provides profiling of the Earth's atmosphere with high vertical resolution and global coverage. This technique has been found to enhance weather forecasting and climate monitoring. Also, ionospheric and space weather application. In this paper, we validate 13 years of the GPS RO temperature and vapor pressure profiles of COSMIC satellite mission over Egypt with those of the

available six RS stations. In general, we find a very good agreement between two techniques with mean temperature bias for all stations equal (0.22) with standard deviation (1.83). According to pressure level sorting into 4 groups, the change of temperature mean bias and standard deviation are increasing with the pressure level decreasing, this might be due to the greater spatial differences between GPS RO events and RS stations. In the overall comparison statistics of temperature differences and the number of matched observations at each pressure level we found that the number of matched observations was small at the top of atmosphere and at the at the lower tropospheric layers, this is due to the

available RS data is decreasing in the top layer depends on the average height of a balloon burst. And a little information from GPS RO data because it does not reach to the surface due to the atmospheric reflection and multipath effects in the lower troposphere. We split daytime and nighttime temperature differences to specify the radiation bias and we found that the mean of temperature differences was below (0.1) for most atmospheric pressure levels with standard deviation was below (1.1).

Mean vapor pressure bias for all stations equal (-0.02) with standard deviation (0.12). The difference between the two techniques is very small, nearly zero in the upper tropopause and stratosphere, where the effects of water vapor are insignificant. The small variation of statistical analysis indicated that the vapor pressure of RS and GPS RO agree very well. There are no distinct variations between daytime and nighttime differences may be because the small number of matched observations. From our results we suggest that more studying need to be done to investigate the temperature and vapor pressure errors other than radiation errors from RS and GPS RO techniques such as calibration, time lag, data processing errors, and study the effect of other meteorological parameters and conditions between two techniques to improve the quality of meteorological research.

References

- [1] Nations, United. 2015. "Human Security: Building Resilience to Climate Threats." United Nations Trust Fund for Human Security 4.
- [2] Steig, Eric J., David P. Schneider, Scott D. Rutherford, Michael E. Mann, Josefino C. Comiso, and Drew T. Shindell. 2009. "Warming of the Antarctic Ice-Sheet Surface since the 1957 International Geophysical Year." *Nature* 457(7228):459–62. doi: 10.1038/nature07669.
- [3] Bein, Thomas, Christian Karagiannidis, and Michael Quintel. 2020. "Climate Change, Global Warming, and Intensive Care." *Intensive Care Medicine* 46(3):485–87. doi: 10.1007/s00134-019-05888-4.
- [4] Council, Natural Environment Research. 2020. "Why Is Climate Important? - NCAS." National Centre for Atmospheric Science.
- [5] Ho, S. P., L. Peng., and H. Vömel. (2017). Characterization of the long-Term radiosonde temperature biases in the upper troposphere and lower stratosphere using COSMIC and Metop-A/GRAS data from 2006 to 2014. *Atmospheric Chemistry and Physics*, 17(7), 4493– 4511.
- [6] Ho, S. P., X. Zhou., X. Shao., B. Zhang., L. Adhikari., S. Kireev., Y. He, J. G. Yoe., W. XiaSerafino., and E. Lynch. (2020). Initial assessment of the COSMIC-2/FORMOSAT-7 neutral atmosphere data quality in NESDIS/STAR using in situ and satellite data. *Remote Sensing*, 12(24), 1–21.
- [7] Ho, S. P., X. Zhou., Y. H. Kuo., D. Hunt., and J. Wang. (2010). Global evaluation of radiosonde water vapor systematic biases using GPS radio occultation from COSMIC and ECMWF analysis. *Remote Sensing*, 2(5), 1320–1330.
- [8] Ho, S. P., Y. H. Kuo., and S. Sokolovskiy. (2007). Improvement of the temperature and moisture retrievals in the lower troposphere using AIRS and GPS radio occultation measurements. *Journal of Atmospheric and Oceanic Technology*, 24(10), 1726–1739.
- [9] Eyre, J. R. (n.d.). An introduction to GPS radio occultation and its use in NWP. Paper presented at GRAS SAF workshop on Application of GPS radio occultation measurements; ECMWF, June 2008, 16– 18.
- [10] Norman, R., Le Marshall, J., Zhang, K., Wang, C. S., Carter, B. A., Rohm, W., ... & Li, Y. (2014). Comparing GPS Radio Occultation Observations with Radiosonde Measurements in the Australian Region. In *Earth on the Edge: Science for a Sustainable Planet* (pp. 51-57). Springer, Berlin, Heidelberg.
- [11] Ware, R., M. Exner, D. Feng, M. Gorbunov, K. Hardy, B. Herman, Y. Kuo, T. Meehan, W. Melbourne, C. Rocken, W. Schreiner, S. Sokolovskiy, F. Solheim, X. Zou, R. Anthes, S. Businger, and K. Trenberth (1996), GPS Sounding of the atmosphere from Low Earth Orbit: Preliminary results, *Bull. Am. Meteorol. Soc.*, 77, 19-40.
- [12] Kursinski, E. R., Hajj, G. A., Hardy, K. R., Romans, L. J., and Schofield, J. T. (1995). Observing tropospheric water vapor by radio occultation using the Global Positioning System, *Geophysical Research Letters*, 22, 2365-2368.
- [13] Kursinski, E. R., Hajj, G. A., Hardy, K. R., Schofield, J. T., and Linfield, R. (1997), Observing earth's atmosphere with radio occultation measurements. *J. Geophys. Res.*, 102, 23429–23465.
- [14] Rocken, C., and Ware, R. (1997), Near real-time GPS sensing of atmospheric water vapor. *Geophys. Res. Lett.* 24 (24), 3221–3224.
- [15] Rossiter, D. (2003). Comparison Between GPS Radio Occultation and Radiosonde Sounding Data.
- [16] Kuo, Y. H., Schreiner, W. S., Wang, J., Rossiter, D. L., and Zhang, Y. (2005). Comparison of GPS radio occultation soundings with radiosondes, *Geophysical Research Letters*, 32, 4.
- [17] Zhang, K., B. Biadegligne, F. Wu, Y. Kuleshov, A. Rea, G.de Hodet, & E. Fu., (2007). A Comparison of Atmospheric Temperature and Moisture Profiles Derived from GPS radio Occultation and Radiosone in Australia. The 3rd Workshop for Space, Aeronautical and Navigational Electronics,

November.

[18] Kishore, P., Venkat R. M., Namboothiric, S. P., Velicognaa, I., Bashab, G., Jiang, J. H., Igarashi, K., Rao, S. V. B., and Sivaku- mar, V. (2011). Global (50°S–50°N) Distribution of water vapour ob- served by Cosmic GPS Ro: comparison with GPS Radiosonde, NCEP, Era-Interim, and Jra-25 reanalysis data sets, *J. Atmos. Sol.-Terr. Phy.*, 73, 1849–1860.

[19] Wang, B. R., X. Y. Liu, and J. K. Wang. (2013). Assessment of COSMIC Radio Occultation Retrieval Product Using Global Radiosonde Data. *Atmospheric Measurement Techniques* 6(4): 1073–83.

[20] Xu, G., X. Yue, W. Zhang., and X. Wan., (2017). Assessment of atmospheric wet profiles obtained from COSMIC radio occultation observations over China. *Atmosphere*, 8(11).

[21] Khaniani, A. S. (2020). Long-Term Evaluation of Temperature Profiles Derived from Space-Based GPS Meteorology with Radiosonde Measurements over Iran. 4(1): 1–12pp.

[22] Li, Y., Y. Yuan., and X. Wang. (2020). Assessments of the Retrieval of Atmospheric Profiles from GNSS Radio Occultation Data in Moist Tropospheric Conditions Using Radiosonde Data. *Remote Sensing* 12(17).

[23] Mousa, A. K., Y. Aoyama, and T. Tsuda. (2006). A Simulation Analysis to Optimize Orbits for a Tropical GPS Radio Occultation Mission. *Earth, Planets and Space* 58(8): 919–25pp.

[24] Ghoniem, I. F., A. K. Mousa, and G. El-Fiky. (2017). Distribution of the GNSS-LEO Occultation Events over Egypt. *NRIAG Journal of Astronomy and Geophysics* 6(1):

97–103pp.

[25] Ghoniem, I. F., A. K. Mousa, and G. El-Fiky. (2020). GNSS-RO LEO Satellite Orbit Optimization for Egypt and the Middle East Region. *Alexandria Engineering Journal* 59(1): 389–97 pp.

[26] Ao, C., Chan, T., Iijima, B., & Li, J. (2008). Planetary boundary layer information from GPS radio occultation measurements. *GRAS SAFWorkshop on Applications of GPSRO Measurements*, 16-18 June 2008, June, 123–131.

[27] Sun, B., Reale, A., Schroeder, S., Seidel, D. J., & Ballish, B. (2013). Toward improved corrections for radiation-induced biases in radiosonde temperature observations. *Journal of Geophysical Research Atmospheres*, 118(10), 4231–4243.

[28] Yu, X., Xie, F., & Ao, C. O. (2018). Evaluating the lower-tropospheric COSMIC GPS radio occultation sounding quality over the Arctic. *Atmospheric Measurement Techniques*, 11(4), 2051–2066.